



RESEARCH LETTER

10.1002/2015GL067070

Key Points:

- Volcanic sulfate significantly affects cloud droplet radius
- The North Atlantic cloud droplet radius was at its all time minimum from the observational record
- GCMs appear to underestimate the effect of tropospheric sulfate on cloud properties

Supporting Information:

- Figures S1–S4

Correspondence to:

D. T. McCoy,
dtmccoy@atmos.uw.edu

Citation:

McCoy, D. T., and D. L. Hartmann (2015), Observations of a substantial cloud-aerosol indirect effect during the 2014–2015 Bárðarbunga-Veiðivötn fissure eruption in Iceland, *Geophys. Res. Lett.*, 42, 10,409–10,414, doi:10.1002/2015GL067070.

Received 18 NOV 2015

Accepted 21 NOV 2015

Accepted article online 1 DEC 2015

Published online 11 DEC 2015

Observations of a substantial cloud-aerosol indirect effect during the 2014–2015 Bárðarbunga-Veiðivötn fissure eruption in Iceland

Daniel T. McCoy¹ and Dennis L. Hartmann¹¹Atmospheric Sciences Department, University of Washington, Seattle, Washington, USA

Abstract The Bárðarbunga-Veiðivötn fissure eruption lasted from 31 August 2014 to 28 February 2015, during which its sulfur emissions dwarfed anthropogenic emissions from Europe. This natural experiment offers an excellent opportunity to investigate the aerosol indirect effect and the effect of effusive volcanic eruptions on climate. During the eruption cloud droplet effective radius (r_e) over the region surrounding Iceland was at the lowest value in the 14 year Moderate Imaging Spectroradiometer data record during September and October 2014. The change in reflected solar radiation due to increased cloud reflectivity during September and October is estimated to exceed 2 W m^{-2} over the region surrounding Iceland, with increases of 1 W m^{-2} extending as far south as the Açores. The strength of the aerosol indirect effect diagnosed here reaffirms the ability of volcanic aerosols to affect cloud properties and ultimately the planetary albedo.

1. Introduction

Cloud-aerosol indirect effects remain a central source of model uncertainty in the representation of anthropogenic climate change [Intergovernmental Panel on Climate Change, 2013]. Understanding the contribution of natural aerosols to cloud brightening [Twomey, 1977] allows us to better understand the effect of anthropogenic aerosols on climate during the industrial period and to better constrain climate sensitivity [Carslaw et al., 2013]. Volcanic sources of cloud condensation nuclei (CCN) are thought to provide one of the primary sources of CCN in the preindustrial era [Schmidt et al., 2012].

Distinguishing natural aerosol indirect effects from other sources of variability in cloud properties is often difficult. The effects of some natural sources of CCN can be discerned because their sources follow distinct spatial or temporal patterns and analysis of data over large regions can reveal their effects on cloud properties [McCoy et al., 2015; Meshkizde and Nenes, 2006; Vallina et al., 2006]. Volcanoes offer a challenge to this type of analysis because their eruptions are irregular and may only persist for a few days. This makes it difficult to disentangle the natural variability in cloud properties from volcanic aerosol indirect effects in the troposphere. Further complicating matters, volcanic emissions may be advected a significant distance from their source [Schmidt et al., 2015]. Attributing cloud changes to volcanic aerosols over short time scales and at a distance from the eruption is extremely difficult. Previous studies of volcanic aerosols on cloud properties either had to utilize global models [Gettelman et al., 2015; Rap et al., 2013; Schmidt et al., 2012] or study the downwind plume from continuously degassing volcanoes [Ebmeier et al., 2014; Gassó, 2008; Yuan et al., 2011]. These studies establish the capacity for volcanic emissions to affect cloud properties.

In this study we present remote sensing observations during the Bárðarbunga-Veiðivötn fissure eruption showing the effects of a substantial amount of sulfur dioxide (SO_2) on the North Atlantic cloud properties. We will focus on the first indirect effect whereby hygroscopic particles decrease the droplet effective radius (r_e) and lead to an enhancement in cloud albedo [Twomey, 1977].

The eruption of the Bárðarbunga-Veiðivötn fissure in 2014–2015 offers an excellent opportunity to evaluate indirect effects from volcanic aerosols. The eruption begun 31 August 2014 and lasted until 28 February 2015 [Schmidt et al., 2015; Sigmundsson et al., 2015]. The volcanic plume exceeded 3000 m above ground level [Schmidt et al., 2015]. Twenty to one hundred and twenty kilotons a day of SO_2 were emitted during the eruption, dwarfing regional anthropogenic sources and making the eruption the largest in Iceland in the past two centuries [Gettelman et al., 2015; Schmidt et al., 2015]. In the atmosphere SO_2 reacts to form sulfate aerosol, which is an effective cloud condensation nuclei (CCN) [Boucher and Lohmann, 1995; Jones et al., 1994].

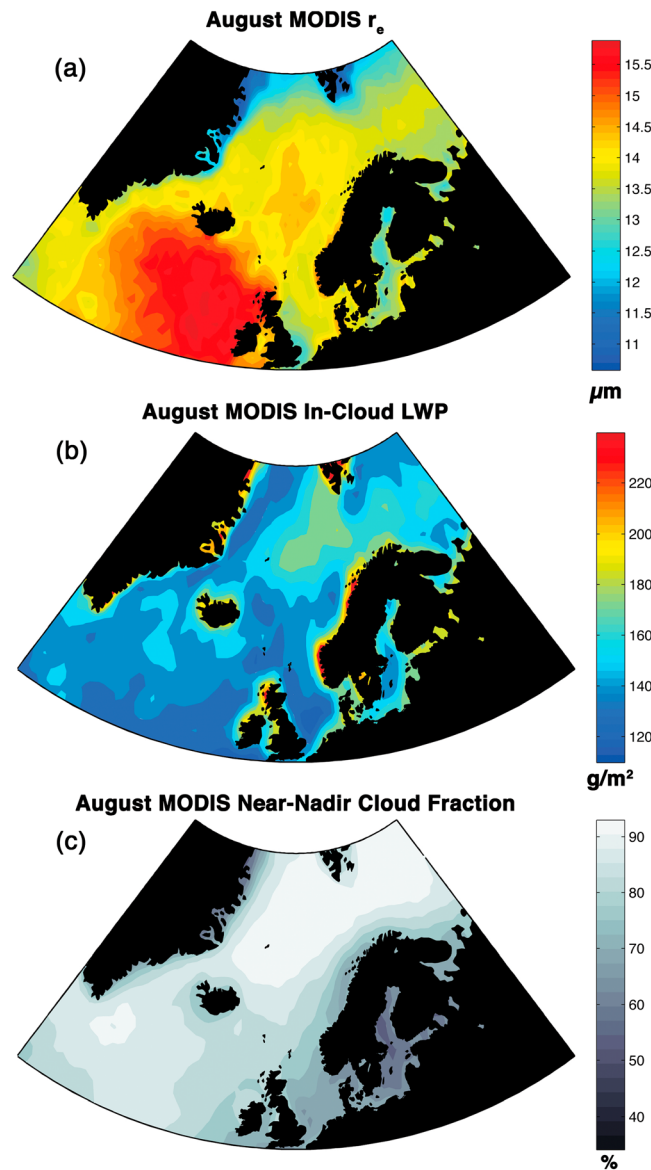


Figure 1. The cloud properties near Iceland from August 2014. (a) The cloud droplet effective radius (r_e), (b) the cloud liquid water path, and (c) the retrieved cloud fraction at near-nadir view angles [Maddux et al., 2010]. Maps are the average of the Terra and Aqua retrievals.

This combination of a substantial source of SO_2 and the lengthy eruptive period makes the Bárðarbunga-Veiðivötn eruption ideal for estimating the volcanic first indirect effect. In addition to the quantity and persistence of emissions, the Bárðarbunga-Veiðivötn fissure erupted in a region with extensive cloud cover that could be affected by the volcanic aerosol (Figure 1). The large spatial and temporal influence of the volcano provided a large sample of affected cloud to be measured by the Moderate Imaging Spectroradiometer (MODIS) instrument that flies aboard the Aqua and Terra platforms [Platnick et al., 2003]. These observations described the changes to cloud microphysics during the eruptive period.

2. Methods

Cloud properties were described using the MODIS Collection 6 data from the instruments aboard the Aqua and Terra platforms [Baum et al., 2012; King et al., 2006]. CERES data were taken from the Clouds and Earth's Radiant Energy Systems (CERES) EBAF2.8r data set [Kato et al., 2013; Loeb et al., 2009]. CERES is used in this study to estimate the climatological clear-sky SW and is only used to estimate the change in SW due to perturbations in cloud properties. Level 3 monthly mean data were used for both the CERES and MODIS data. All data were resolved at a horizontal resolution of $1^\circ \times 1^\circ$. Cloud optical properties are retrieved using the MODIS instrument. Cloud droplet effective radius (r_e) and liquid water path (LWP) were retrieved for clouds that

were determined to be liquid topped by MODIS. Ice water path (IWP) was retrieved for clouds that were determined to be ice topped. Additional data describing anomalies detected when only data from single-layer clouds were used are supplied in the supporting information.

3. Results

The cloud droplet effective radius in the region surrounding Iceland is relatively constant and only varies spatially by a few micron (Figure 1). The anthropogenic cloud-aerosol indirect effect in this region is estimated to be relatively small by climate models [Chuang et al., 2002; Rap et al., 2013; Zelinka et al., 2013].

In the summer preceding the eruption, only small local anomalies in r_e were detected relative to the climatological record spanning 2001–2015 (Figures 2 and S1–3 in the supporting information). The introduction of sulfur from the Bárðarbunga-Veiðivötn fissure beginning in September 2014 coincides with a decrease in r_e across the

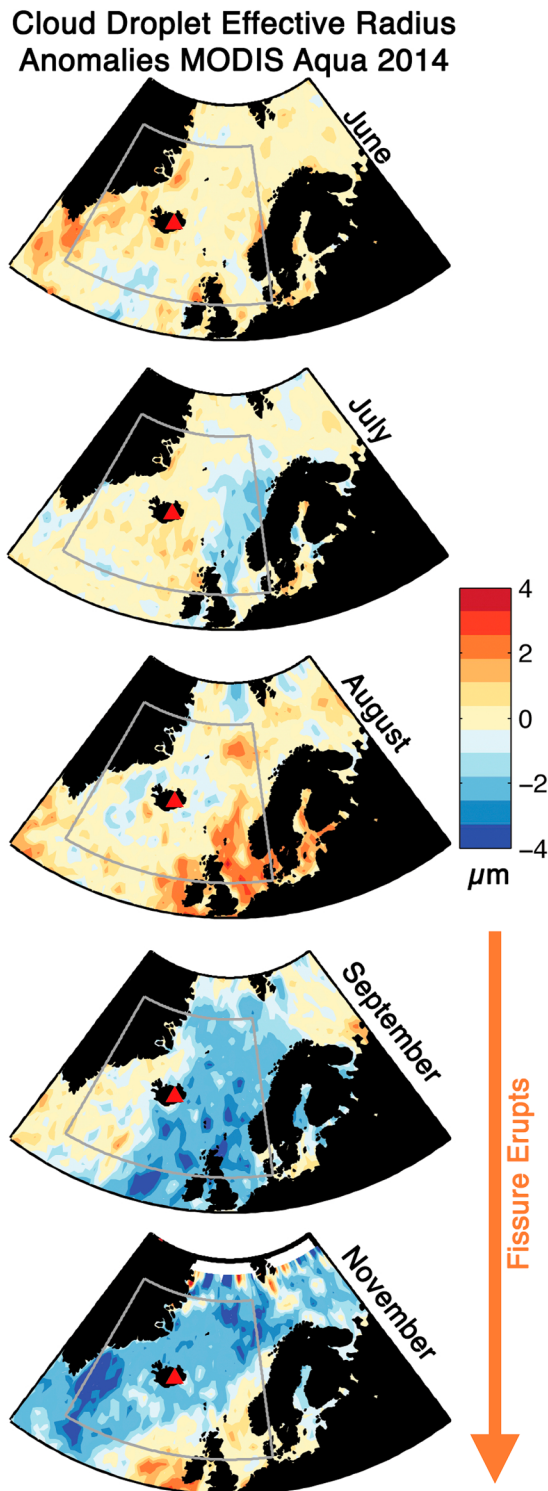


Figure 2. Anomalies in cloud droplet effective radius (r_e) from 2014 before and during the Bárðarbunga-Veiðivötn fissure eruption (31 August). Anomalies are from the Aqua instrument retrieved using the 2.1 μm retrieval band and are computed relative to the climatology. The location of Bárðarbunga-Veiðivötn is shown using a red triangle. During October the solar zenith angle was sufficiently high in some regions that no reliable cloud property retrievals could be made by MODIS. These regions are left blank. The study area (40°W – 10°E and 55°N – 75°N) used in Figure 3 is outlined in grey.

North Atlantic between Greenland and Scandinavia in excess of $4\ \mu\text{m}$ relative to the climatological r_e . This decrease in r_e is consistent with the first indirect effect increasing cloud droplet number concentration at a constant liquid water content [Twomey, 1977]. Unfortunately, the solar zenith angle and illumination during the winter (November through February) are such that MODIS cannot retrieve cloud properties across the North Atlantic. For the remainder of this work we will focus on volcanic activity and cloud properties in September and October 2014 when the eruption was most powerful [Schmidt et al., 2015].

During September and October 2014 negative anomalies in r_e in excess of $4\ \mu\text{m}$ from the mean of $\sim 16\ \mu\text{m}$ were observed. Sustained anomalies of $-2\ \mu\text{m}$ extended over large areas of the ocean near Iceland (Figures 2 and S1–3). The patterns of anomalies during September and October are consistent with the atmospheric flow over Iceland (Figure S4). It is interesting to note that these anomalies are similar in magnitude to the biogenic CCN-driven seasonal cycle of r_e across the Southern Ocean [Ayers and Gras, 1991; Kruger and Grassl, 2011; McCoy et al., 2014; McCoy et al., 2015; Meskhidze and Nenes, 2006; Vallina et al., 2006].

The cloud droplet effective radius in the ocean surrounding Iceland (40°W – 10°E and 55°N – 75°N) during September and October 2014 were the lowest observed during the MODIS data record (Figure 3). These decreases in the r_e represented a three standard deviation decrease relative to observed variability, and they appear independently in the observations made by the MODIS instruments aboard the Aqua and Terra satellites and in all three of the retrieval bands used by MODIS to measure r_e (Figure 3). Because the clouds during months of the eruption are so different from any other months during the period of observations, it seems unlikely that weather anomalies played a significant role, but it is possible that they have some small influence, certainly in

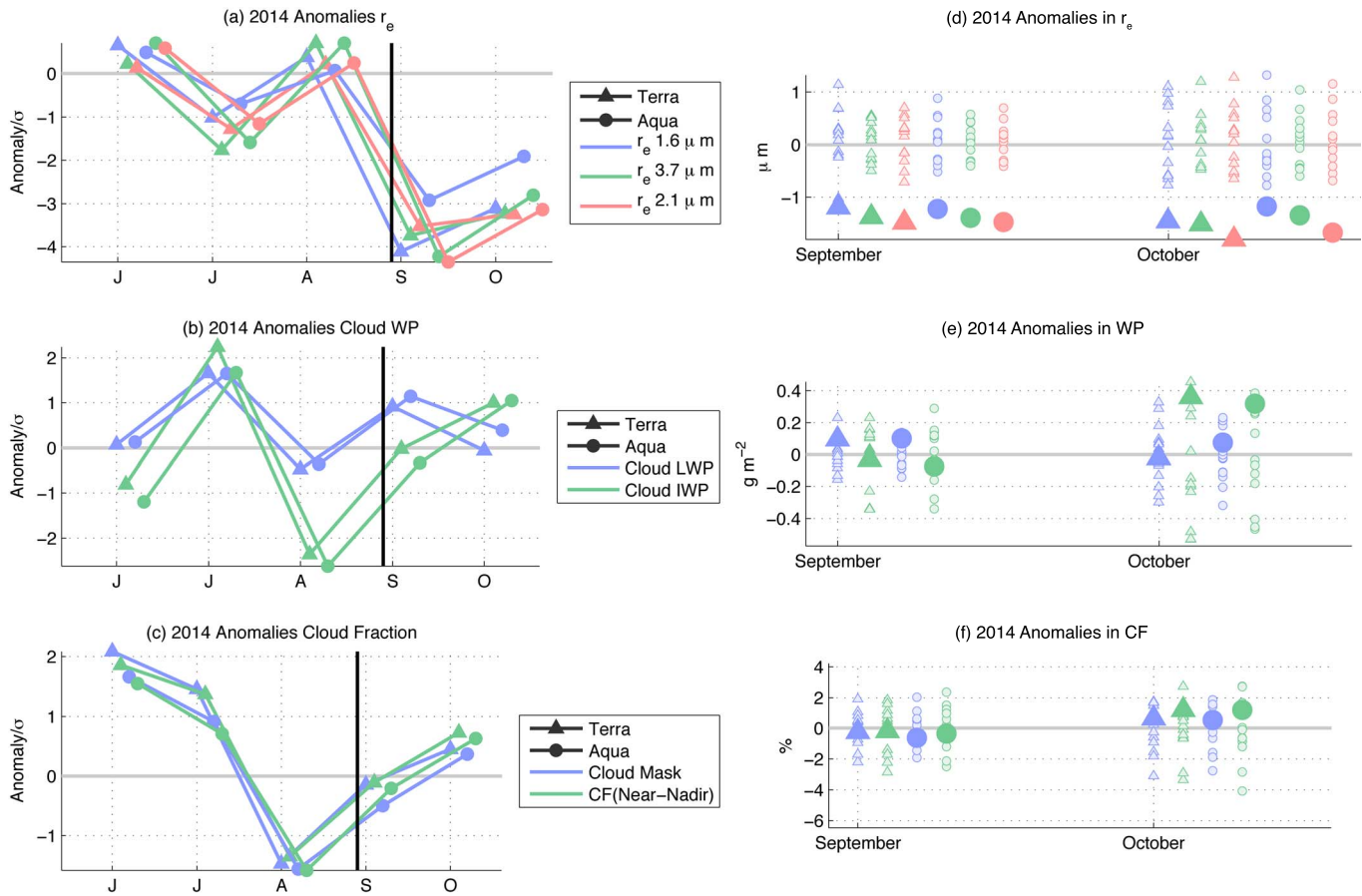


Figure 3. The time series of anomalies in various cloud properties over the study region 40°W–10°E and 55°N–75°N (see Figure 2) during 2014. (a–c) Anomalies are shown normalized by the standard deviation of the climatology from 2002 to 2015, excluding 2014. (d–f) Anomalies are shown for September and October of every year in the observational record and anomalies during the eruption are shown as filled symbols. The horizontal position of the monthly means is shifted slightly for visual clarity. In Figures 3a–3c the beginning of the eruption is noted as a black vertical line in each plot. Each month shows the anomalies detected by Terra (triangles) and Aqua (circles) separately. Figures 3a and 3d show anomalies in cloud droplet effective radius (r_e) as detected using the 1.6 μm , 2.1 μm , and 3.7 μm retrieval bands. Figures 3b and 3e show anomalies in cloud LWP and IWP. Figures 3c and 3f show anomalies in cloud fraction using both the MODIS cloud mask and the cloud fraction measured at near-nadir view angles [Maddux et al., 2010].

the positioning of the cloud response relative to the volcano. We might expect increases in both LWP and cloud cover contingent on increasing CCN [Albrecht, 1989; Lebsock et al., 2008]. Cloud fraction and liquid water path (LWP) were examined but did not show appreciable changes (Figure 3).

To put the anomalies in r_e detected by MODIS in the context of the global energy budget, we will offer an idealized estimate of the change reflected SW due to enhancement in cloud albedo. The SW absorbed at the surface is decreased due to this enhanced reflectivity. This calculation is carried out assuming that cloud fraction (CF) and LWP are well represented by the observed climatology. As in previous studies [Charlson et al., 1992; McCoy et al., 2015; Meskhidze and Nenes, 2006], we estimate the change in cloud albedo for some perturbation to r_e , assuming an adiabatic cloud with vertically uniform cloud droplet number concentration, as

$$\Delta\alpha_c = \frac{1}{3} \times \alpha_c \times (1 - \alpha_c) \times \left[1 - \frac{r_{e1}^3}{r_{e0}^3} \right] \quad (1)$$

and the change in upwelling SW as

$$\Delta\text{SW}_\uparrow = \text{SW}_\uparrow \times \text{CF} \times \Delta\alpha_c \quad (2)$$

where SW_\uparrow is the downwelling SW at cloud top, estimated using the climatological clear-sky downwelling SW at the surface estimated from CERES. Cloud fraction (CF) is the product of climatological near-nadir cloud

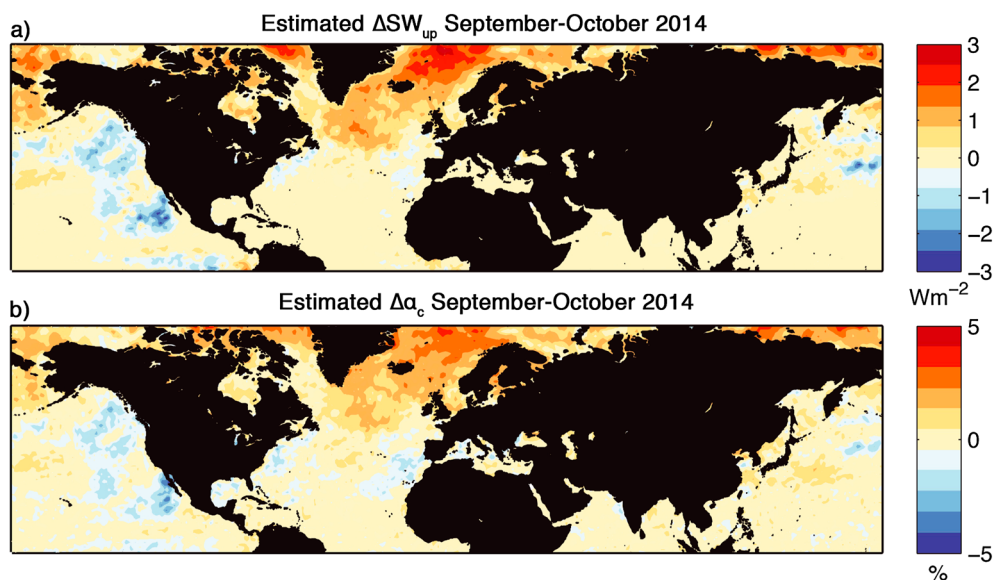


Figure 4. The estimated change in (a) upwelling SW and (b) cloud albedo estimated from the anomalies in cloud droplet effective radius from the 2.1 μm retrieval band for September and October 2014 and climatological liquid cloud properties. Note that in Figure 4a an increase in upwelling SW implies a decrease in SW reaching the surface. Latitudes north of 75°N have been excluded because no retrievals were available in October. Differences in upwelling SW are given in W m^{-2} , and cloud albedo is given in absolute percent.

fraction from MODIS [Maddux *et al.*, 2010] and the fraction of clouds identified as liquid topped by MODIS. Cloud albedo (α_c) is estimated using the MODIS liquid cloud optical depth retrieval. The perturbed and climatological effective radii are shown as r_{e1} and r_{e0} , respectively. This estimate is somewhat conservative for two reasons. (1) The downwelling SW is likely to be somewhat larger at cloud top than at the surface because it has been less attenuated. (2) Using liquid topped, only cloud cover assumes that any liquid clouds that are obscured by overlying ice cloud are not changing their r_e .

The estimated changes in upwelling SW and cloud albedo over the first 2 months of the eruption due to anomalies in r_e are shown in Figure 4. Cloud albedo was estimated to increase by up to 3% in the Norwegian Sea and Greenland Sea (Figure 4b). Local increases in upwelling SW exceeded 2 W m^{-2} . The zonal mean upwelling SW across the 60°N–70°N latitude band was estimated to increase by 1 W m^{-2} , and the cloud albedo was estimated to increase by 1.5% (Figure 4).

Events such as Bárðarbunga-Veiðivötn allow us to examine strong perturbations to cloud microphysics and refine our understanding of the aerosol indirect effect and the effect of effusive volcanic emissions on climate. Comparison between the MODIS record and simulations coupled to a MODIS simulator [Bodas-Salcedo *et al.*, 2011] would provide a useful testing ground for the evaluation of simulated aerosol indirect effects. This may allow cloud-aerosol indirect effects to be better constrained.

Acknowledgments

The authors wish to thank Annica Ekman, Ilona Riipinen, and Lexie Goldberger for their discussion, guidance, and advice. Johannes Mohrmann provided extensive technical support using the HYSPLIT package. The authors also wish to thank the organizers and lecturers of the Advanced Climate Dynamics Course summer school held in Laugarvatn, Iceland, in August 2015. Finally, we thank the two anonymous reviewers for useful comments and advice. The authors were supported under NASA grant NNX14AG26G.

References

- Albrecht, B. A. (1989), Aerosols, cloud microphysics, and fractional cloudiness, *Science*, 245(4923), 1227–1230.
- Ayers, G. P., and J. L. Gras (1991), Seasonal relationship between cloud condensation nuclei and aerosol methanesulphonate in marine air, *Nature*, 353(6347), 834–835.
- Baum, B. A., W. P. Menzel, R. A. Frey, D. C. Tobin, R. E. Holz, S. A. Ackerman, A. K. Heidinger, and P. Yang (2012), MODIS cloud-top property refinements for collection 6, *J. Appl. Meteorol. Climatol.*, 51(6), 1145–1163.
- Bodas-Salcedo, A., *et al.* (2011), COSP: Satellite simulation software for model assessment, *Bull. Am. Meteorol. Soc.*, 92(8), 1023–1043.
- Boucher, O., and U. Lohmann (1995), The sulfate-CCN-cloud albedo effect, *Tellus B*, 47(3), 281–300.
- Carlsaw, K. S., *et al.* (2013), Large contribution of natural aerosols to uncertainty in indirect forcing, *Nature*, 503(7474), 67–71.
- Charlson, R. J., S. E. Schwartz, J. M. Hales, R. D. Cess, J. A. Coakley, J. E. Hansen, and D. J. Hofmann (1992), Climate forcing by anthropogenic aerosols, *Science*, 255(5043), 423–430.
- Chuang, C. C., J. E. Penner, J. M. Prospero, K. E. Grant, G. H. Rau, and K. Kawamoto (2002), Cloud susceptibility and the first aerosol indirect forcing: Sensitivity to black carbon and aerosol concentrations, *J. Geophys. Res.*, 107(D21), 4564, doi:10.1029/2000JD000215.
- Ebmeier, S. K., A. M. Sayer, R. G. Grainger, T. A. Mather, and E. Carboni (2014), Systematic satellite observations of the impact of aerosols from passive volcanic degassing on local cloud properties, *Atmos. Chem. Phys.*, 14(19), 10,601–10,618.

- Gassó, S. (2008), Satellite observations of the impact of weak volcanic activity on marine clouds, *J. Geophys. Res.*, *113*, D14S19, doi:10.1029/2007JD009106.
- Gottelman, A., A. Schmidt, and J. Egill Kristjánsson (2015), Icelandic volcanic emissions and climate, *Nat. Geosci.*, *8*(4), 243–243.
- Intergovernmental Panel on Climate Change (2013), *Climate Change 2013: The Physical Science Basis. Contribution of Working Group I to the Fifth Assessment Report of the Intergovernmental Panel on Climate Change*, 1535 pp., Cambridge Univ. Press, Cambridge, U. K., and New York.
- Jones, A., D. L. Roberts, and A. Slingo (1994), A climate model study of indirect radiative forcing by anthropogenic sulfate aerosols, *Nature*, *370*(6489), 450–453.
- Kato, S., N. G. Loeb, F. G. Rose, D. R. Doelling, D. A. Rutan, T. E. Caldwell, L. S. Yu, and R. A. Weller (2013), Surface irradiances consistent with CERES-derived top-of-atmosphere shortwave and longwave irradiances, *J. Clim.*, *26*(9), 2719–2740.
- King, M. D., S. Platnick, P. A. Hubanks, G. T. Arnold, E. G. Moody, G. Wind, and B. Wind (2006), Collection 005 change summary for the MODIS cloud optical property (06_OD) algorithm, *MODIS Atmos.*, *8*.
- Kruger, O., and H. Grassl (2011), Southern Ocean phytoplankton increases cloud albedo and reduces precipitation, *Geophys. Res. Lett.*, *38*, L08809, doi:10.1029/2011GL047116.
- Lebsack, M. D., G. L. Stephens, and C. Kummerow (2008), Multisensor satellite observations of aerosol effects on warm clouds, *J. Geophys. Res.*, *113*, D15205, doi:10.1029/2008JD009876.
- Loeb, N. G., B. A. Wielicki, D. R. Doelling, G. L. Smith, D. F. Keyes, S. Kato, N. Manalo-Smith, and T. Wong (2009), Toward optimal closure of the Earth's top-of-atmosphere radiation budget, *J. Clim.*, *22*(3), 748–766.
- Maddux, B. C., S. A. Ackerman, and S. Platnick (2010), Viewing geometry dependencies in MODIS cloud products, *J. Atmos. Oceanic Technol.*, *27*(9), 1519–1528.
- McCoy, D. T., D. L. Hartmann, and D. P. Grosvenor (2014), Observed Southern Ocean cloud properties and shortwave reflection. Part I: Calculation of SW flux from observed cloud properties, *J. Clim.*, *27*(23), 8836–8857.
- McCoy, D. T., S. M. Burrows, R. Wood, D. P. Grosvenor, S. M. Elliott, P.-L. Ma, P. J. Rasch, and D. L. Hartmann (2015), Natural aerosols explain seasonal and spatial patterns of Southern Ocean cloud albedo, *Sci. Adv.*, *1*(6), e1500157.
- Meskhidze, N., and A. Nenes (2006), Phytoplankton and cloudiness in the Southern Ocean, *Science*, *314*(5804), 1419–1423.
- Platnick, S., M. D. King, S. A. Ackerman, W. P. Menzel, B. A. Baum, J. C. Riedi, and R. A. Frey (2003), The MODIS cloud products: Algorithms and examples from Terra, *IEEE Trans. Geosci. Remote Sens.*, *41*(2), 459–473.
- Rap, A., C. E. Scott, D. V. Spracklen, N. Bellouin, P. M. Forster, K. S. Carslaw, A. Schmidt, and G. Mann (2013), Natural aerosol direct and indirect radiative effects, *Geophys. Res. Lett.*, *40*, 3297–3301, doi:10.1002/grl.50441.
- Schmidt, A., K. S. Carslaw, G. W. Mann, A. Rap, K. J. Pringle, D. V. Spracklen, M. Wilson, and P. M. Forster (2012), Importance of tropospheric volcanic aerosol for indirect radiative forcing of climate, *Atmos. Chem. Phys.*, *12*(16), 7321–7339.
- Schmidt, A., et al. (2015), Satellite detection, long-range transport, and air quality impacts of volcanic sulfur dioxide from the 2014–2015 flood lava eruption at Bárðarbunga (Iceland), *J. Geophys. Res. Atmos.*, *120*, 9739–9757, doi:10.1002/2015JD023638.
- Sigmundsson, F., et al. (2015), Segmented lateral dyke growth in a rifting event at Bar[eth]arbunga volcanic system, Iceland, *Nature*, *517*(7533), 191–195.
- Twomey, S. (1977), Influence of pollution on shortwave albedo of clouds, *J. Atmos. Sci.*, *34*(7), 1149–1152.
- Vallina, S. M., R. Simo, and S. Gasso (2006), What controls CCN seasonality in the Southern Ocean? A statistical analysis based on satellite-derived chlorophyll and CCN and model-estimated OH radical and rainfall, *Global Biogeochem. Cycles*, *20*, GB1014, doi:10.1029/2005GB002597.
- Yuan, T., L. A. Remer, and H. Yu (2011), Microphysical, macrophysical and radiative signatures of volcanic aerosols in trade wind cumulus observed by the A-Train, *Atmos. Chem. Phys.*, *11*(14), 7119–7132.
- Zelinka, M. D., S. A. Klein, K. E. Taylor, T. Andrews, M. J. Webb, J. M. Gregory, and P. M. Forster (2013), Contributions of different cloud types to feedbacks and rapid adjustments in CMIP5*, *J. Clim.*, *26*(14), 5007–5027.